Absolute frequency measurement of sub-Doppler molecular lines using a 3.4-μm difference-frequency-generation spectrometer and a fiber-based frequency comb

Keisuke Takahata,[1,2] Takumi Kobayashi,[1,3] Hiroyuki Sasada,[1,2] Yoshiaki Nakajima,[3,4] Hajime Inaba,[3] and Feng-Lei Hong[3]

[1]*Department of Physics, Faculty of Science and Technology, Keio University, 3-14-1 Hiyoshi, Kohoku-ku, Yokohama 223-8522, Japan*

[2]*Sentan, Japan Science and Technology Agency, Sanbancho 5, Chiyoda-ku, Tokyo 102–0075, Japan*

[3]*National Institute of Advanced Industrial Science and Technology (AIST), Tsukuba Central 3, 1-1-1 Umezono, Tsukuba, Ibaraki 305-8563, Japan*

[4]*Graduate School of Engineering, University of Fukui, 3-9-1 Bunkyo, Fukui 910-8507, Japan*

We measure the absolute frequency of 12 sub-Doppler lines of the $P(6)$ and $P(7)$ transitions in the ν_3 band of $^{12}CH_4$ using difference-frequency-generation (DFG) of 1.064-μm Nd:YAG and 1.55-μm DFB lasers and a fiber-based frequency comb referenced to International Atomic Time. The relative uncertainties are typically 9.4×10^{-11}, and the determined value for the $P(7)$ $F_2^{(2)}$ line agrees with the International Committee for Weights and Measures recommendation with a discrepancy of (1.2 ± 8.4) kHz. The combination of the DFG spectrometer and the frequency comb enables determining energy levels as accurately as microwave spectroscopy.

PACS number(s): 33.20.Ea, 42.62.Eh, 06.30.Ft, 07.57.Ty

I. INTRODUCTION

Nonlinear saturated absorption spectroscopy is usually employed in atomic spectroscopy to enhance spectral resolution from the order of 10^{-6} for Doppler-limited spectroscopy to the order of 10^{-8} for sub-Doppler resolution spectroscopy [1]. Typical extended-cavity laser diodes in the visible and near-infrared regions provide sufficient power with a spectral linewidth narrower than the natural linewidth of the electronic transition for sub-Doppler resolution spectroscopy. The laser frequency stabilized to the Lamb dip can be precisely measured with an optical frequency comb based on a mode-locked Ti:sapphire laser (Ti:s comb) linked to a Cs atomic clock.

Sub-Doppler resolution spectroscopy has also been applied for molecular vibration-rotation transitions in the mid-infrared region. Indeed, an accidental frequency coincidence between a 3.39-μm He-Ne laser and the $F_2^{(2)}$ component of the $P(7)$ transition in the ν_3 band of $^{12}CH_4$ was used to resolve 1-kHz recoil splittings corresponding to a relative resolution of 1.2×10^{-11} [2], and provides a recommended radiation for realization of the definition of the meter [3]. In the 10 μm region, microwave sideband CO_2 laser spectrometers [4] have been applied to sub-Doppler resolution spectroscopy of more than 10 molecular species, and in the 5 μm region, a similar spectrometer has been developed using a CO laser [5]. In general, however, sub-Doppler resolution is not attained in molecular vibrational spectroscopy due to a lack of radiation sources with a linewidth narrower than 1 MHz and an output power level larger than 0.1 mW because mid-infrared lasers have not been developed so remarkably as visible and near-infrared lasers. Furthermore, the source must be widely tunable in order to observe the entire molecular vibrational band usually extending over a few terahertz.

A tunable 3-μm source for saturated absorption spectroscopy is eagerly anticipated for the investigation of the fundamental vibrational bands of the CH, NH, and OH stretching modes. Sub-Doppler resolution molecular spectroscopy provides fundamental information of vibration-rotation interactions in molecular physics, which is also useful for various fields such as metrology, environmental science, and astronomy. Thus far Lamb dips of the ν_3 band of $^{12}CH_4$ and $^{13}CH_4$ have been observed using a He-Ne laser [2,6] and an optical parametric oscillator [7], but the He-Ne laser is poorly tunable and the optical parametric oscillator is not continuously tunable. Difference-frequency generation (DFG) in periodically poled lithium niobate (PPLN) has been applied to a widely and continuously tunable source in the 3 μm region and employed in sub-Doppler resolution spectroscopy [8–10]. In particular, we recently demonstrated that a DFG spectrometer containing an efficient ridge waveguide PPLN [11,12] enabled us to record deep Lamb dips with a width of a few hundreds kHz using compact pump and signal sources and a simple absorption cell [10].

The DFG source has advantages over mid-infrared lasers in not only the tunability but also frequency calibration: the absolute frequency of the DFG source can be precisely determined by measuring the frequencies of the pump and signal sources using an optical frequency comb based on a mode-locked erbium-doped fiber laser (fiber comb) [13,14] covering the wavelength range of 0.95 to 2.2 μm or a Ti:s comb for 0.5 to 1.1 μm. Thus far, the absolute frequency of a Doppler-broadened absorption line in the ν_3 band of $^{12}CH_4$ has been measured using a DFG source and a fiber comb [15]. Recently, DFG of a fiber comb provided the 3.4-μm frequency comb, which was phase-coherently connected with a methane-stabilized He-Ne laser [16]. In the 4.2-μm region, the absolute frequency of a saturated absorption line in the ν_3 band of CO_2 was measured using a DFG source and a Ti:s comb [17]. The frequency of a 4.3-μm quantum cascade laser was stabilized to the Lamb dip of a CO_2 line and measured using a Ti:s comb and nonlinear sum-frequency generation [18].
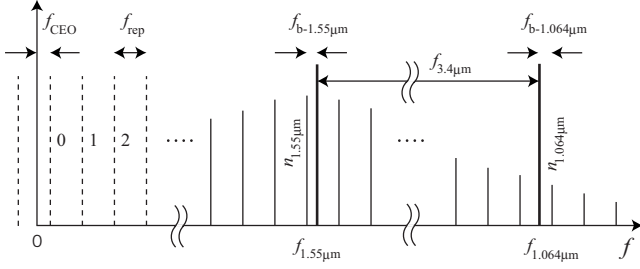
FIG. 1. Schematic of frequency measurement of the 3.4-μm idler wave generated from the 1.064-μm pump and 1.55-μm signal waves using optical frequency comb.

In this work, we stabilized the frequency of the 3.4-μm DFG source [10] to saturated absorption lines of ^{12}CH$_4$, and determined the absolute frequency using a fiber comb. The present measurement also verifies for the first time, as far as we know, that the combination of the DFG spectrometer and the fiber comb is widely tunable over 300 GHz where all 12 tetrahedral components of the $P(6)$ and $P(7)$ transitions scatter. They involve the $F_2^{(2)}$ and E components of the $P(7)$ transition whose absolute frequencies were precisely measured with the He-Ne laser and a frequency chain [3,19]. A comparison with our result is useful for evaluating the present measurement. For the other 10 components beyond the tunable range of the He-Ne laser, this is the first absolute frequency measurement in a sub-Doppler resolution, and the results are important for investigation of vibration-rotation interactions and useful for precise spectroscopy as frequency references and detection of trace gas.

II. FREQUENCY MEASUREMENT WITH OPTICAL FREQUENCY COMB

Figure 1 presents the frequency-measurement scheme. The frequency of the fiber comb is calculated as

$$f_n = nf_{\text{rep}} + f_{\text{CEO}}, \qquad (1)$$

where n is the number of the comb mode, and f_{rep} and f_{CEO} are the repetition rate and the carrier-envelope offset frequency [20]. They are phase-locked to a hydrogen (H) maser frequency reference linked to the International Atomic Time

(TAI). The frequencies of the 1.064-μm ($f_{1.064\,\mu\text{m}}$) and 1.55-μm ($f_{1.55\,\mu\text{m}}$) lasers are given in terms of the signed beat frequencies, $f_{\text{b}-1.064\,\mu\text{m}}$ and $f_{\text{b}-1.55\,\mu\text{m}}$, as

$$f_{1.064\,\mu\text{m}} = n_{1.064\,\mu\text{m}}f_{\text{rep}} + f_{\text{CEO}} + f_{\text{b}-1.064\,\mu\text{m}} \qquad (2)$$

and

$$f_{1.55\,\mu\text{m}} = n_{1.55\,\mu\text{m}}f_{\text{rep}} + f_{\text{CEO}} + f_{\text{b}-1.55\,\mu\text{m}}. \qquad (3)$$

Therefore, the 3.4-μm frequency is determined by

$$
\begin{aligned}
f_{3.4\,\mu\text{m}} &= f_{1.064\,\mu\text{m}} - f_{1.55\,\mu\text{m}} \\
&= (n_{1.064\,\mu\text{m}} - n_{1.55\,\mu\text{m}})f_{\text{rep}} + f_{\text{b}-1.064\,\mu\text{m}} - f_{\text{b}-1.55\,\mu\text{m}},
\end{aligned}
$$
$$(4)$$

which is insensitive to f_{CEO}.

Figure 2 illustrates the schematic diagram of the measurement. A DFG source consists of a ridge waveguide PPLN (NEL, model WD-3360–000-A-B-C) with a conversion efficiency of 9%/W, a 1.55-μm distributed feedback (DFB) laser diode (NEL, model NLK1C6DAAA) with a nominal spectral linewidth of 60 kHz as a signal source, a fiber amplifier, and a 1.064-μm iodine-stabilized Nd:YAG laser with a nominal spectral linewidth of 5 kHz as a pump source [21–23]. The signal (80 mW) and pump (60 mW) waves are combined by an optical fiber coupler and led into the PPLN. The generated 3.4-μm idler wave of 0.4 mW is collimated by two lenses and passes through a CaF$_2$ plate and a 50-cm-long absorption cell, which is fitted with quartz windows and filled with 1.3-Pa methane. The beam waist of 0.74 mm radius is located at the middle of the cell, and the Rayleigh length is 50 cm. The transmitted idler wave is sent back to the cell by a flat mirror, then partly reflected by the CaF$_2$ plate, and detected by a liquid-nitrogen-cooled InSb photodiode. The wavefront curvature of the counterpropagating waves is larger than 1.0 m. We did not deliberately change idler power, beam alignment, or sample pressure during the whole measurement. Sweeping the idler frequency by changing the injection current of the DFB laser, the transmission spectrum is recorded with a digital oscilloscope. The Lamb dip is 0.25–0.4 MHz wide (HWHM) and a few percent deep relative to the Doppler-broadened line [10]. The spectral width is estimated 140 kHz from the transit time and the curvature of
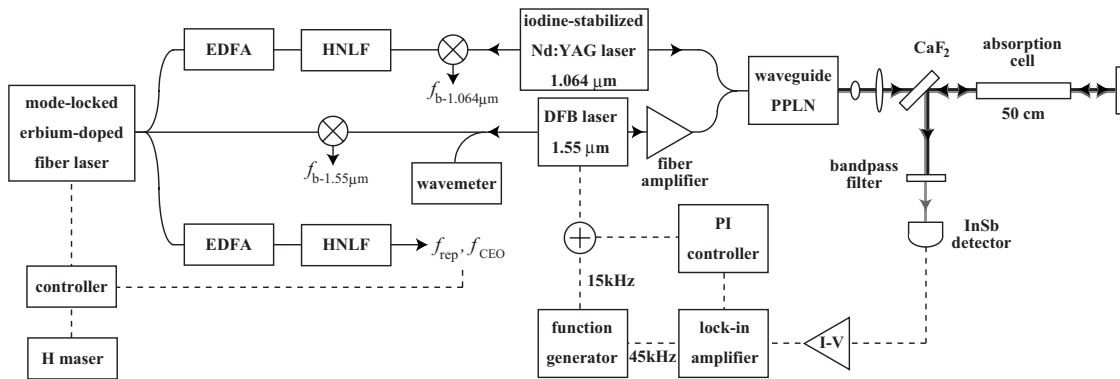

FIG. 2. Schematic diagram of the experiment setup. EDFA: Erbium-doped fiber amplifier, HNLF: Highly nonlinear fiber, PI: Proportional-integrating, I-V: Current to voltage converter.

the wave front, 30 kHz from pressure broadening, and 60 kHz from the light source. Hence, the hyperfine structures due to the protons (~10 kHz) are not resolved. To stabilize the idler frequency to the Lamb dip, the idler frequency is modulated in a depth of about 2 MHz peak-to-peak by adding a 15-kHz sinusoidal signal to the injection current of the DFB laser. The detected signal is phase-sensitively demodulated at 45 kHz ($3f$ detection) by a lock-in amplifier, and the output is fed back as an error signal to the injection current of the DFB laser through a proportional-integrating (PI) controller.

One tenth of the signal and pump power is sent to a fiber comb. A mode-locked fiber laser oscillates at 1.56 μm at a repetition rate f_{rep} of 121 MHz, and the output is divided into three branches. The first and second branches are used to detect the beat notes between the fiber combs and the pump and signal waves. The fiber laser output and the carrier-envelope offset beat note are detected in the third branch, and the frequencies are phase-locked to each rf frequency reference synthesized from a H maser linked to the TAI. The first and third branches contain an erbium-doped fiber amplifier (EDFA) and a highly nonlinear fiber (HNLF) [24] in order to broaden the comb spectrum. All the beat notes have a signal-to-noise ratio exceeding 40 dB at a 300-kHz bandwidth, which is sufficient for phase-locking and frequency counting. The details of the fiber comb are similar to that used in previous works [23,25].

The idler frequency $f_{3.4\,\mu m}$ stabilized to the Lamb dips of the methane lines is derived from Eq. (4) independent of f_{CEO}. However, we phase-lock f_{CEO} to the rf reference in the present measurement in order to maintain $f_{b-1.064\,\mu m}$ and $f_{b-1.55\,\mu m}$ within a frequency bandwidth of an electric bandpass filter. The value of $n_{1.064\,\mu m}$ in Eq. (2) is determined from the absolute frequency of the iodine-stabilized Nd:YAG laser [22], and that of $n_{1.55\,\mu m}$ from wavelength measurement using a wavemeter with a resolution of about 1 GHz and the HITRAN 2004 database [26]. The values of $f_{b-1.064\,\mu m}$ and $f_{b-1.55\,\mu m}$ are simultaneously counted with two dead-time-free counters. The counter gate time is 1s, while each measurement is implemented over a period of 450 to 720 s. The sign of the beat notes is determined by slightly changing f_{rep} and f_{CEO}. Figure 3 indicates the normalized Allan deviation for the $F_2^{(2)}$ component of the $P(7)$ transition. It is 8×10^{-11} at 1-s averaging time, and reduces to the 8×10^{-12} level at 100-s averaging time. The frequency stability of the present measurement is limited by the methane-stabilized idler wave because the iodine-stabilized Nd:YAG laser, the H maser, and the fiber comb have frequency stabilities (Allan deviations) better than 1×10^{-12} at 1-s averaging time [23].

III. RESULT AND DISCUSSIONS

Table I lists results of the absolute frequency measurements together with discrepancies from the previous measurements [3,19,26]. The tetrahedral components in Table I are for the vibrational ground state, and the mid-infrared transition occurs between the $A_1 \leftrightarrow A_2$, $F_1^{(i)} \leftrightarrow F_2^{(i)}$, and $E \leftrightarrow E$ components, where i is 1 or 2. The average of the standard deviations is 8.3 kHz except for the E components of the
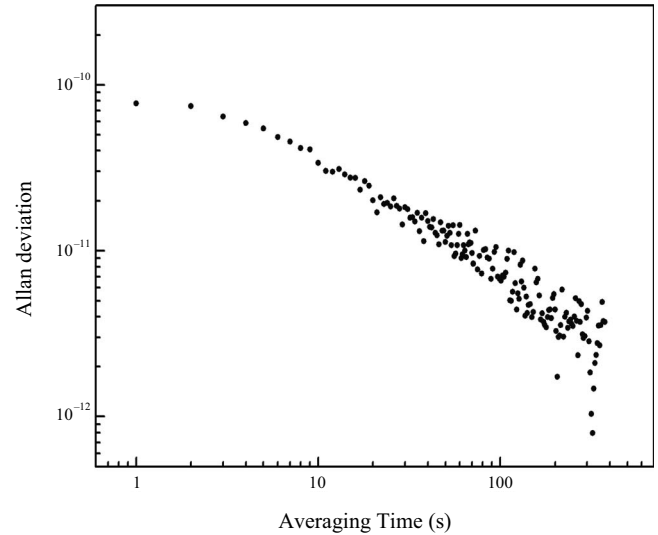

FIG. 3. Allan deviation of the 3.4-μm idler frequency stabilized to the $F_2^{(2)}$ component of the $P(7)$ transition.

$P(7)$ transition for which the $3f$ signal is noisier than those for the others. This value corresponds to the 1-s measurements and is expected to reduce for longer measurements because the Allan deviation in Fig. 3 decreases as the averaging time increases longer than 1 s. The measured frequency for the $F_2^{(2)}$ component of the $P(7)$ transition agrees with International Committee for Weights and Measures (CIPM) recommendation for the hyperfine-unresolved line [3] with a discrepancy of (1.2 ± 8.4) kHz. To evaluate the reproducibility, we measured the frequency of the same component twice on the next day, and the measured values were slightly larger than the CIPM recommendation by (2.0 ± 7.0) and (4.1 ± 8.3) kHz. For the other components, the frequency measurement was carried out once, and the result improves the HITRAN 2004 database [26] by two orders of magnitude.

(i) Pressure shift, (ii) wavefront curvature and intensity imbalance in the counterpropagating beams [27], (iii) frequency modulation [28], and (iv) beam crossing and misalignment [29] give rise to systematic shift in the sub-Doppler line center. (i) According to the HITRAN 2004 database [26], the pressure shift coefficients of the measured transitions are between -0.15 to -0.50 MHz/Torr. The pressure shift for the experimental condition of 10 mTorr (1.3 Pa) is thus estimated less than 5 kHz, which is within the typical standard deviation. (ii) The reflected beam has the smallest wavefront curvature of about 1 m at the source-side cell window, where the intensity imbalance in the incident and reflected beams also takes the largest value of 2.5. Even at this position, the frequency shift is expected less than 5 kHz [27]. Because the observed saturated absorption signal was integrated over the cell length, the resultant frequency shift is much smaller than the standard deviations. (iii) The frequency modulation characteristics of the 1.55-μm DFB laser may depend on the wavelength. We did not find any appreciable asymmetry of the error signal (the third derivative of saturated absorption spectrum), but we did not investigate it quantitatively. (iv) The light source based on the fiber-linked

TABLE I. Measured and reference frequencies of the v_3 band of $^{12}CH_4$. Meas.: Measured, Ref.: Reference. The numbers in parentheses are uncertainties in unit of the last digit.

Transition	Component	Measured frequency (kHz)	Standard deviation (kHz)	Reference frequency (kHz)	(Measured)–(Reference) frequency (kHz)
$P(7)$	$F_1^{(2)}$	88368863353.9	9.4	88368862.43×10^3 [a]	0.92×10^3
	E	88373149015.7	40.1	$88373149028.55(20)$ [b]	-12.8
	$F_2^{(2)}$	88376181601.7	8.4	$88376181600.5(20)$ [c]	1.2
	A_2	88382052724.0	5.9	88382052.10×10^3 [a]	0.62×10^3
	$F_2^{(1)}$	88391450564.4	8.7	88391449.57×10^3 [a]	0.99×10^3
	$F_1^{(1)}$	88393030001.9	11.9	88393029.66×10^3 [a]	0.34×10^3
$P(6)$	A_1	88679126631.3	4.0	88679124.69×10^3 [a]	1.94×10^3
	F_1	88682207769.3	8.6	88682206.53×10^3 [a]	1.24×10^3
	$F_2^{(2)}$	88685592321.5	7.1	88685590.37×10^3 [a]	1.95×10^3
	A_2	88694688778.6	8.8	88694685.12×10^3 [a]	3.66×10^3
	$F_2^{(1)}$	88698120466.4	7.7	88698120.11×10^3 [a]	0.36×10^3
	E	88699071286.0	11.1	88699070.57×10^3 [a]	0.72×10^3

[a]Reference [26].
[b]Reference [19].
[c]CIPM recommended value [3].

single-mode waveguide emits a symmetric output beam, and the pointing direction changed $\delta\theta \sim 3 \times 10^{-5}$ radian at most in the tuning range of the spectrometer of 300 GHz. Even if the residual Doppler shift was induced by optical misalignment, the magnitude of the observed transitions varies less than about 4 kHz.

Even though methane is a nonpolar molecule, rotational and vibrational motions may induce small electric dipole moments and thereby rotational transitions. Six microwave transitions in the vibrational ground and $v_3 = 1$ states related to the mid-infrared transitions in Table I were observed, and the relevant energy level diagram is illustrated in Fig. 4. The transition frequencies were measured to be $E_{6,7,F_2^{(1)}}^{v_3=1} - E_{6,7,F_1^{(2)}}^{v_3=1} = (15\ 601.846 \pm 0.0010)$ MHz [30]
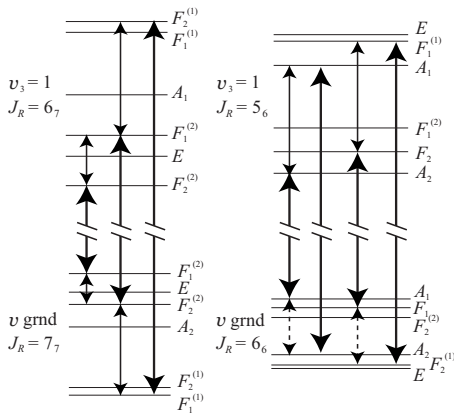

FIG. 4. Level diagram for the measured mid-infrared transitions and the associated microwave transitions. Those drawn in a solid line are frequency measured while those in a doted line have not been observed. The energy scale in the vibrational ground state is ten times larger than that in the $v_3 = 1$ state.

$E_{7,7,F_2^{(2)}}^{ground} - E_{7,7,F_1^{(1)}}^{ground} = (1\ 246.55 \pm 0.02)$ MHz [31], $E_{6,7,F_1^{(2)}}^{v_3=1} - E_{6,7,F_2^{(2)}}^{v_3=1} = (6\ 895.204 \pm 0.010)$ MHz [30], $E_{7,7,F_2^{(2)}}^{ground} - E_{7,7,F_2^{(2)}}^{ground} = (423.02 \pm 0.02)$ MHz [32], $E_{5,6,F_1^{(1)}}^{v_3=1} - E_{5,6,F_2^{(1)}}^{v_3=1} = (15\ 126.853 \pm 0.012)$ MHz [33], and $E_{5,6,A_1}^{v_3=1} - E_{5,6,A_2}^{v_3=1} = (14\ 801.356 \pm 0.018)$ MHz [33], where $E_{J,R,\Gamma}^{v}$ is the energy of the level with total angular momentum quantum number J, rotational angular momentum quantum number R, tetrahedral component Γ, and vibrational state v. The microwave frequencies are associated with the mid-infrared frequencies as

$$(E_{6,7,F_2^{(1)}}^{v_3=1} - E_{6,7,F_1^{(2)}}^{v_3=1}) + (E_{7,7,F_2^{(2)}}^{ground} - E_{7,7,F_1^{(1)}}^{ground})$$
$$= (E_{6,7,F_2^{(1)}}^{v_3=1} - E_{7,7,F_1^{(1)}}^{ground}) - (E_{6,7,F_1^{(2)}}^{v_3=1} - E_{7,7,F_2^{(2)}}^{ground}) \quad (5)$$

and

$$(E_{6,7,F_1^{(2)}}^{v_3=1} - E_{6,7,F_2^{(2)}}^{v_3=1}) + (E_{7,7,F_1^{(2)}}^{ground} - E_{7,7,F_2^{(2)}}^{ground})$$
$$= (E_{6,7,F_1^{(2)}}^{v_3=1} - E_{7,7,F_2^{(2)}}^{ground}) - (E_{6,7,F_2^{(2)}}^{v_3=1} - E_{7,7,F_1^{(2)}}^{ground}). \quad (6)$$

Substituting the measured values into Eqs. (5) and (6), the discrepancies between the left and right sides are 4.2 and 23.8 kHz, which are likely limited by the uncertainty of microwave spectroscopy. Similarly, two rf transition frequencies in the vibrational ground state are predicted as

$$E_{6,6,A_1}^{ground} - E_{6,6,A_2}^{ground} = 760\ 791.3 \pm 18.4\ kHz$$

and

$$E_{6,6,F_1}^{ground} - E_{6,6,F_2^{(1)}}^{ground} = 785\ 844.1 \pm 16.7\ kHz,$$

and the expected uncertainties are again primarily determined by the uncertainty of microwave spectroscopy [33].

Precise molecular energy levels are usually derived from microwave spectroscopy of rotational transitions. The spectral resolution, which is limited by homogeneous broadening, is approximately the same as that of sub-Doppler resolution mid-infrared vibrational spectroscopy. However, it is easier for microwave spectroscopy to determine the frequency with an uncertainty corresponding to the spectral resolution than for mid-infrared spectroscopy because the microwave frequency is approximately by three order of magnitude lower than the mid-infrared frequency: thus, the frequency measurement system requires lower relative accuracy. In this work, we have demonstrated that the combination of the DFG spectrometer and the fiber comb considerably expands the wavelength range where both sub-Doppler resolution and the corresponding frequency uncertainty can be obtained. Therefore, the rotational structure in the vibrational excited states can be determined with the same precision as those in the vibrational ground state and thermally populated vibrational excited states. This development is important in particular for nonpolar molecules because in principle they have no rotational transitions and accurate spectroscopic data have to be obtained from mid-infrared spectroscopy.

The tunable range of the DFG spectrometer is temporarily limited to 400 GHz which is the temperature tuning range of the single 1.55-μm DFB laser. A ridge waveguide PPLN can be used to generate 3.2 to 3.6 μm radiation, and the single device works within a 2-THz frequency span by changing the temperature for the phase matching [10]. Therefore, we are able to perform precise vibrational spectroscopy over the entire 3.4 μm region by replacing the 1.55-μm source and the ridge waveguide PPLN.

IV. SUMMARY

We have determined the absolute frequencies of 12 sub-Doppler spectral lines of methane in the 3.4 μm region beyond the tunable range of the He-Ne laser with a typical uncertainty of 8.3 kHz. The DFG source and the fiber comb are a promising combination for highly accurate molecular spectroscopy in the mid-infrared region.

ACKNOWLEDGMENTS

[1] W. Demtröder, *Laser Spectroscopy* (Springer-Verlag, Berlin, 2003), Chap. 7.

[2] J. L. Hall, C. J. Bordé, and K. Uehara, Phys. Rev. Lett. **37**, 1339 (1976).

[3] T. J. Quinn, Metrologia **40**, 103 (2003).

[4] G. Magerl, J. M. Frey, W. A. Kreiner, and T. Oka, Appl. Phys. Lett. **42**, 656 (1983).

[5] B. Meyer, S. Saupe, M. H. Wappelhorst, T. George, F. Kühnemann, M. Schneider, M. Havenith, W. Urban, and J. Legrand, Appl. Phys. B: Lasers Opt. **61**, 169 (1995).

[6] K. Uehara and J. L. Hall, Opt. Lett. **4**, 214 (1979).

[7] E. V. Kovalchuk, D. Dekorsy, A. I. Lvovsky, C. Braxmaier, J. Mlynek, A. Peters, and S. Schiller, Opt. Lett. **26**, 1430 (2001).

[8] P. Maddaloni, G. Gagliardi, P. Malara, and P. de Natale, Appl. Phys. B: Lasers Opt. **80**, 141 (2005).

[9] K. Anzai, X. M. Gao, H. Sasada, and N. Yoshida, Jpn. J. Appl. Phys. **45**, 2771 (2006).

[10] M. Abe, K. Takahata, and H. Sasada, Opt. Lett. **34**, 1744 (2009).

[11] O. Tadanaga, T. Yanagawa, Y. Nishida, H. Miyazawa, K. Magari, M. Asobe, and H. Suzuki, Appl. Phys. Lett. **88**, 061101 (2006).

[12] D. Richter, P. Weibring, A. Fried, O. Tadanaga, Y. Nishida, M. Asobe, and H. Suzuki, Opt. Express **15**, 564 (2007).

[13] B. R. Washburn, S. A. Diddams, N. R. Newbury, J. W. Nicholson, M. F. Yan, and C. G. Jorgensen, Opt. Lett. **29**, 250 (2004).

[14] T. R. Schibli, K. Minoshima, F. L. Hong, H. Inaba, A. Onae, H. Matsumoto, I. Hartl, and M. E. Fermann, Opt. Lett. **29**, 2467 (2004).

[15] P. Malara, P. Maddaloni, G. Gagliardi, and P. De Natale, Opt. Express **16**, 8242 (2008).

[16] M. A. Gubin, A. N. Kireev, A. V. Konyashchenko, P. G. Kryukov, A. S. Shelkovnikov, A. V. Tausenev, and D. A. Tyurikov, Appl. Phys. B: Lasers Opt. **95**, 661 (2009).

[17] D. Mazzotti, P. Cancio, G. Giusfredi, P. De Natale, and M. Prevedelli, Opt. Lett. **30**, 997 (2005).

[18] S. Borri, S. Bartalini, I. Galli, P. Cancio, G. Giusfredi, D. Mazzotti, A. Castrillo, L. Gianfrani, and P. De Natale, Opt. Express **16**, 11637 (2008).

[19] P. S. Ering, D. A. Tyurikov, G. Kramer, and B. Lipphardt, Opt. Commun. **151**, 229 (1998).

[20] D. J. Jones, S. A. Diddams, J. K. Ranka, A. Stentz, R. S. Windeler, J. L. Hall, and S. T. Cundiff, Science **288**, 635 (2000).

[21] F.-L. Hong, S. A. Diddams, R. Guo, Z.-Y. Bi, A. Onae, H. Inaba, J. Ishikawa, K. Okumura, D. Katsuragi, J. Hirata, T. Shimizu, T. Kurosu, Y. Koga, and H. Matsumoto, J. Opt. Soc. Am. B **21**, 88 (2004).

[22] F.-L. Hong, J. Ishikawa, Y. Zhang, R. Guo, A. Onae, and H. Matsumoto, Opt. Commun. **235**, 377 (2004).

[23] H. Inaba, Y. Daimon, F.-L. Hong, A. Onae, K. Minoshima, T. R. Schibili, H. Matsumoto, M. Hirano, T. Okuno, M. Onishi, and M. Nakazawa, Opt. Express **14**, 5223 (2006).

[24] T. Okuno, M. Onishi, T. Kashiwada, S. Ishikawa, and M. Nishimura, IEEE J. Sel. Top. Quantum Electron. **5**, 1385 (1999).

[25] Y. Nakajima, H. Inaba, Feng-Lei Hong, A. Onae, K. Minoshima, T. Kobayashi, M. Nakazawa, and H. Matsumoto, Opt. Commun. **281**, 4484 (2008).

[26] L. S. Rothman, D. Jacquemart, A. Barbe, D. Chris Benner, M. Birk, L. R. Brown, M. R. Carleer, C. Chackerian, Jr., K. Chance, L. H. Coudert, V. Dana, V. M. Devi, J.-M. Flaud, R. R. Gamache, A. Goldman, J.-M. Hartmann, K. W. Jucks, A. G.

Maki, J.-Y. Mandin, S. T. Massie, J. Orphal, A. Perrin, C. P. Rinsland, M. A. H. Smith, J. Tennyson, R. N. Tolchenov, R. A. Toth, J. Vander Auwera, P. Varanasi, and G. Wagner, J. Quant. Spectrosc. Radiat. Transf. **96**, 139 (2005).

[27] J. L. Hall and C. J. Bordé, Appl. Phys. Lett. **29**, 788 (1976).

[28] A. Czajkowski, A. A. Madej, and P. Dubé, Opt. Commun. **234**, 259 (2004).

[29] S. E. Park, H. S. Lee, T. Y. Kwon, and H. Cho, Opt. Commun. **192**, 49 (2001).

[30] M. Takami, K. Uehara, and K. Shimoda, Jpn. J. Appl. Phys. **12**, 924 (1973).

[31] R. F. Curl, Jr., J. Mol. Spectrosc. **48**, 165 (1973).

[32] R. F. Curl, T. Oka, and D. S. Smith, J. Mol. Spectrosc. **46**, 518 (1973).

[33] C. J. Pursell and D. P. Weliky, J. Mol. Spectrosc. **153**, 303 (1992).